Potential investigation of cloud-aerosol interaction with a multiple-wavelength Raman-elastic lidar

Yonghua Wu, Lina Cordero, Chuen-meei Gan, Barry Gross, Fred Moshary, et al.

Yonghua Wu, Lina Cordero, Chuen-meei Gan, Barry Gross, Fred Moshary, Samir Ahmed, "Potential investigation of cloud-aerosol interaction with a multiple-wavelength Raman-elastic lidar," Proc. SPIE 7832, Lidar Technologies, Techniques, and Measurements for Atmospheric Remote Sensing VI, 78320G (26 October 2010); doi: 10.1117/12.865148

SPIE.

Event: SPIE Remote Sensing, 2010, Toulouse, France

Potential investigation of cloud-aerosol interaction with a multiple-wavelength Raman-elastic lidar

Yonghua Wu, Lina Cordero, Chuen-Meei Gan, Barry Gross, Fred Moshary, Sam Ahmed
Optical Remote Sensing Lab, the City College of New York, New York, NY, USA 10031

ABSTRACT

Measurements of low-altitude cloud and its interaction with aerosol are analyzed with a multiple-wavelength elastic-Raman scattering lidar. Using the numerical experiment approach, we first evaluate the retrieval accuracy of cloud extinction from the Raman-lidar algorithms, in particular at the cloud edges. For the low-level water-phase cloud, the simulation also shows the dramatic variation of lidar-ratio, color-ratio and extinction-ratio with the small droplets and their correlation. Then, the measurement examples by CCNY elastic-Raman lidar illustrate that the small droplets probably appear at the cloud edges, which might imply the new particle formation or the cloud-aerosol interaction.

Key words: Cloud, Aerosol, Raman lidar, Color ratio, Lidar ratio

1. INTRODUCTION

Measurement of low-altitude cloud is quite important to investigate cloud-aerosol interaction and their climate effects. Lidar is capable of profiling the cloud-aerosol vertical distribution and hence provides the opportunity to explore the cloud-aerosol optical properties and their interaction [1-3]. Previous researches have indicated that the cloud-aerosol interaction extensively happened at the cloud vicinity or edges with the significant variation of cloud optical properties and droplet size [1-4]. Due to dramatic non-linear or irregular variation of lidar returns by the cloud, the evaluation of lidar algorithm deriving cloud extinction coefficient becomes quite important especially at the cloud edges because the common algorithms may result in the big artificial influence on the retrievals of cloud extinction and extinction-to-backscatter ratio (e.g. lidar ratio or S-ratio) [5-7].

In this paper, we start with the numerical simulation to evaluate the retrieval accuracy of cloud extinction by the Raman lidar. Then, the relationships of water cloud optical properties with the droplet size are simulated which include lidar ratio, color ratio and extinction ratio. Furthermore, the initial analysis of CCNY elastic-Raman lidar measuring water cloud optical properties is illustrated, which indicates the small droplets occurring at the cloud edges and hence implies the potential interaction of cloud and aerosol.

2. METHODOLOGY

A ground-based multi-wavelength elastic-Raman scattering lidar has been operated at New York City (NYC, 40.821°N/73.949°W), as part of Regional East Atmospheric Lidar Mesonet [8, 9]. It emits three laser beams with an Nd: YAG laser at the wavelengths 1064-532-355-nm. Three elastic-scattering returns and two Raman-scattering returns by nitrogen (N_2) and water vapor molecules excited by 355-nm are collected. The receiver telescope has the diameter of 50.8 cm with field of view of 1~2 mrad. The co-axis optical configuration of transmitter and receiver allows the full overlap returns from about 0.5 km altitude. Lidar returns are acquired by LICEL transient recorder (TR40-250, 12-bit 40MHz ADC and 250MHz PC) and recorded with the range resolution of 3.75-m and 1-minute time average.

The combined elastic-Raman returns can be used to derive the particle extinction, backscatter and their ratio at the wavelength 355-nm. To calculate the backscatter at 355-nm, the calibration altitude is chosen above the low cloud if N_2-Raman returns can penetrate the cloud; otherwise the calibration constant under the clear sky patch is

Lidar Technologies, Techniques, and Measurements for Atmospheric Remote Sensing VI,
edited by Upendra N. Singh, Gelsomina Pappalardo, Proc. of SPIE Vol. 7832, 78320G

employed. To process the item $\frac{d}{dz}[\ln\frac{N(z)}{P(\lambda_N,z)z^2}]$ for deriving the extinction from the N_2-Raman lidar equation [5-7], we first make the polynomial regression with $\ln\frac{N(z)}{P(\lambda_N,z)z^2}$ and then estimate the slope of regression. To obtain the cloud backscatter coefficient at wavelength 1064-nm, we first calibrate the lidar system constant with the optically thick water cloud [10-11]; then due to the dominated cloud backscatter comparing with the weak molecular backscatter at 1064-nm, we can estimate the cloud backscatter coefficient with the range-corrected calibrated returns and Raman-channel-derived cloud transmittance. This approach avoids the assumption of lidar ratio and aerosol reference value in the conventional Fernald or Klett algorithm. Once having the backscatter coefficients at 355-nm and 1064-nm, then the color ratio (defined as the ratio of two-wavelength backscatters, β_{1064}/β_{355}) can be obtained, which indicates the particle or droplet size information. As the approximate estimate, cloud extinction at 1064-nm is calculated from the backscatter and lidar-ratio.

3. RESULT AND DISCUSSION

With the numerical experiment approach, we firstly evaluate the influences on the cloud extinction retrieval caused by the algorithms and simulate the variation of color-ratio, lidar-ratio and extinction-ratio with the water cloud droplet diameter. Figure 1 plots the input cloud extinction profile (model or true) and the simulated elastic-Raman scattering lidar returns. As we can see, the N_2-Raman returns at 387-nm show the dramatic non-linear slopes at the cloud edges. In the Raman retrieval equation, we employ the 1-order polynomial (linear), 2-order and 3-order polynomial regressions to derive the item $\frac{d}{dz}[\ln\frac{N(z)}{P(\lambda_N,z)z^2}]$ for cloud extinction coefficient, respectively. Then, the relative differences between the Raman-lidar retrieval and the true (model input) extinction of cloud are estimated. We also simulated the influences caused by the different range resolutions. Figure 2 gives the results. Large bias at the cloud edges can be clearly seen, and the 3-order polynomial regression gives the better accuracy at the cloud top and bottom as seen in the Fig.2a. Meanwhile in the regression, the influences from different spatial resolutions (δz) are also shown in the Fig. 2b. Again, large errors at the cloud top are indicated. The small regression range (δz=90-m) gives the better retrieval. From the above results, the cautions have to be taken to retrieve cloud extinction at the cloud edges, which will be important to investigate the variation of cloud optical properties at the cloud edges because they may result in the large artificial bias.

Water cloud droplets usually are spherical in shape. We can calculate the lidar-ratio, color ratio and extinction ratio at the wavelength pair 1064-355 nm using Mie-theory and a normalized gamma size distribution of water cloud droplet [10]. The model width parameter μ is taken with the values of 1 and 9 which correspond to the range of low-level cloud droplet spectra according to Miles et al. [12]. Figure 3 gives the simulation results. In Figure 3 (a), for the smaller droplet with the diameter less than 2.5 μm, color ratio shows the smaller value and indicates the good correlation with the lidar-ratio. For the droplet diameter of 2.5~25 μm, color ratio varies from 0.2 to 1.3 while the lidar-ratio is almost a constant. In Figure 3(b), the extinction-ratio and lidar-ratio show the negative relationship for the droplets smaller than 2.5 μm in diameter. At the diameter of 2.5~25 μm, extinction ratio varies from 1.0 to 1.4 while the lidar-ratio is almost a constant. Figure 3 indicates that the small droplets show the significantly different optical properties from the large ones and can be discriminated from the lidar-ratio, color-ratio and extinction-ratio. Using the long wavelength such as CO_2 laser, Eberhard [13] verified that water cloud droplet size could be distinguished from the relationship of lidar-ratio and droplet diameter.

We analyze the measurements of low-altitude clouds by the CCNY ground-based multiple-wavelength elastic-Raman lidar. The lidar-ratio and color-ratio of cloud are derived. In the Raman-retrieval of cloud extinction profile, three-order polynomial regression and 90-m range resolution are applied. In calculating the color ratio, we adopt a calibration procedure which uses both high cirrus and low cloud cumulus clouds. As an example, Figure 4 illustrates the lidar results on March 15, 2006. The low-altitude clouds appeared at 2.0-3.0 km altitude as seen in Figure 4(a). Separation of cloud from aerosol is made according to the histogram of backscatter coefficients which is assured by the cloud boundaries masked by the cloud height algorithm. Figure 4 (b) ~ (d) give the backscatter, lidar-ratio and color ratio for the only cloud. First, in the most important part of the cloud layer, the lidar ratio is around 20-sr which is quite consistent with the water cloud optical properties. Second, high lidar ratios occur at the cloud top

edges which are indicative of smaller droplets. Third, small color-ratios also confirm small droplet formation at the cloud top edges.

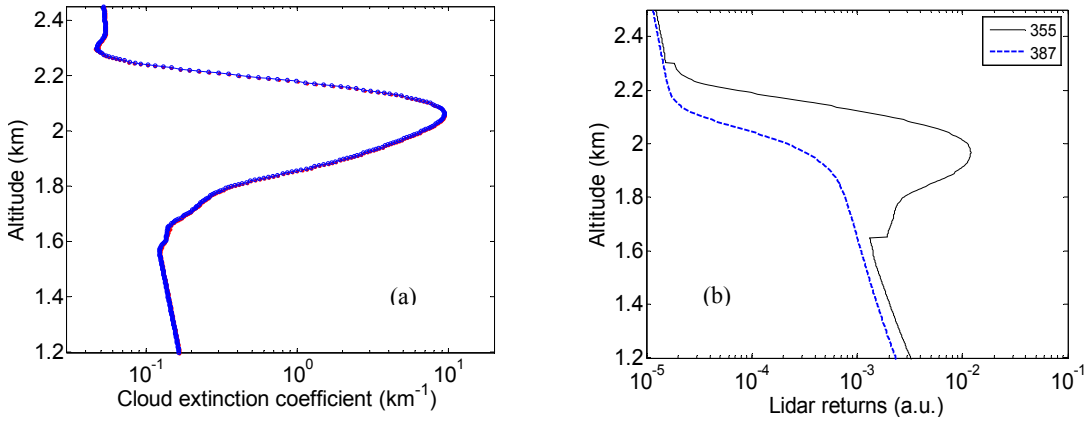

Figure 1. (a) Input cloud extinction profile and (b) simulated elastic and N_2-Raman lidar returns.

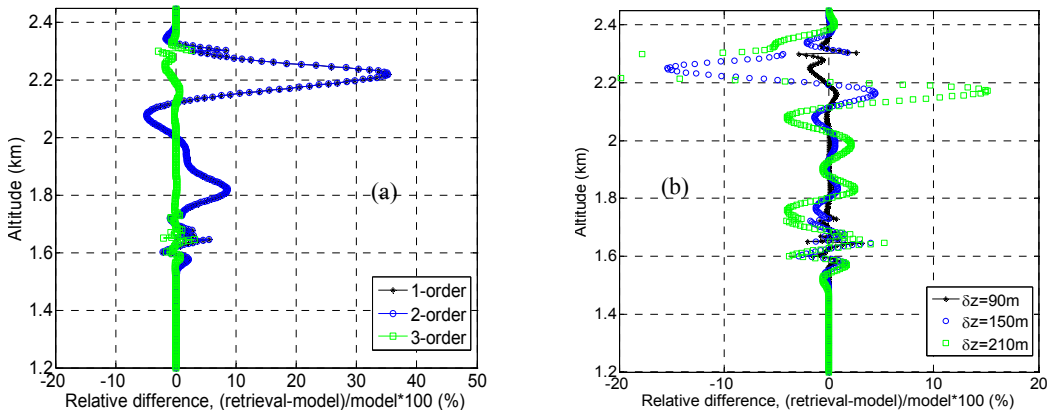

Figure 2. Relative differences of Raman-retrieved cloud extinction from the true values caused by (a) regression methods and (b) spatial resolution.

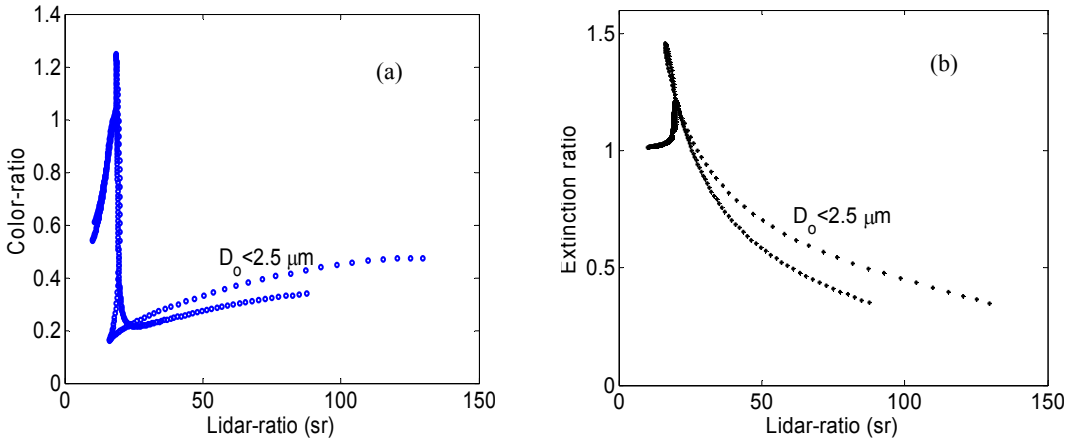

Figure 3. (a) Water cloud color-ratio versus lidar-ratio, and (b) extinction-ratio versus lidar-ratio.

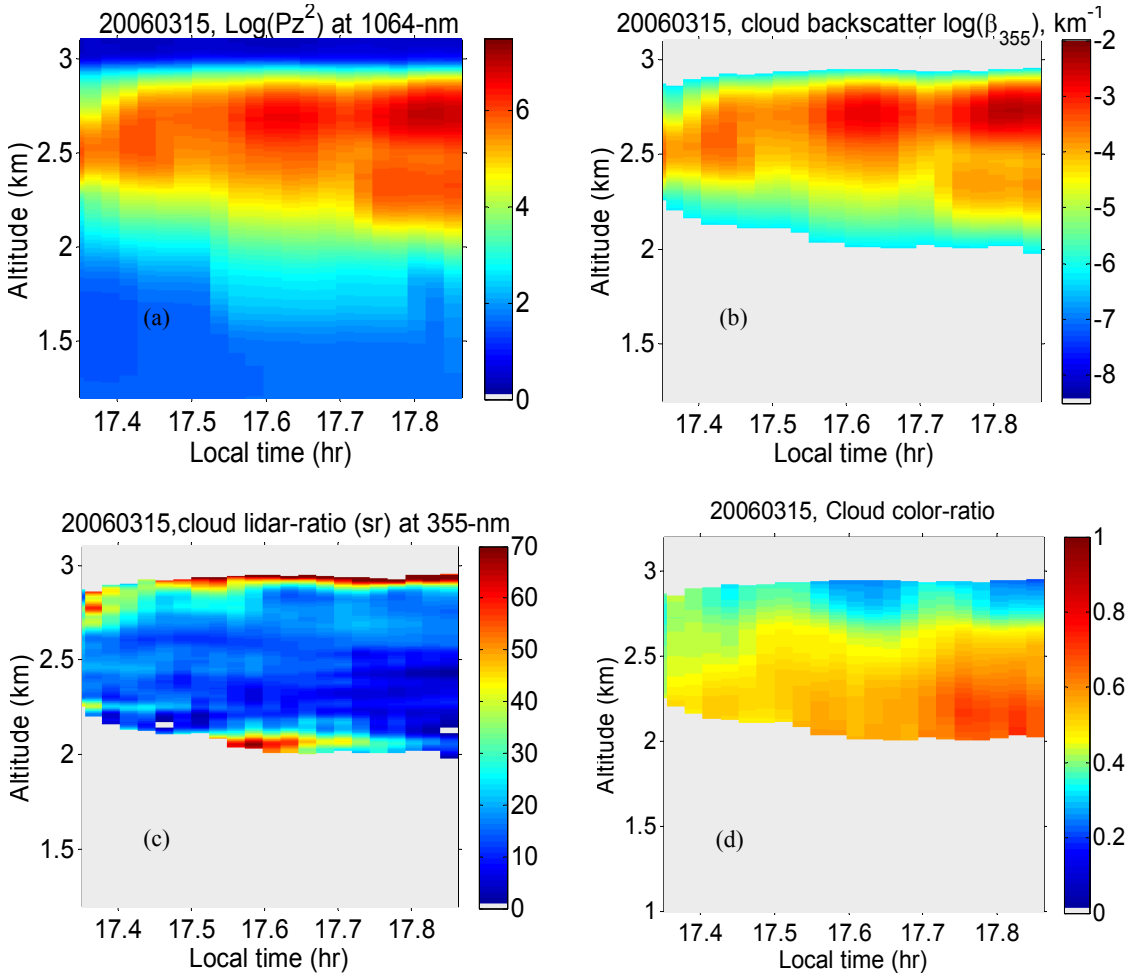

Figure 4. (a) Range-corrected lidar returns at 1064-nm, (b) cloud backscatter coefficient, (c) lidar-ratio and (d) color-ratio on March 15, 2006.

As a second case, Figure 5 (a) gives the cloud lidar-ratio that indicates the large lidar-ratios near the cloud bottom. Meanwhile, as seen in the previous example, the color-ratio and lidar-ratio show the positive correlation at the lower part of cloud in agreement with model predictions (see Fig. 3a). We can also obtain the lidar-ratio below the cloud and explore how the lidar-ratio transitions at the cloud-aerosol interface. As an example, for the same day as above, we calculate the lidar-ratio profile across the cloud as a function of altitude. The cloud base is defined based on histogram analysis which is in good agreement to the location where the backscatter grows very rapidly. We note in particular a smooth transition of the lidar-ratio below cloud about 50 meters where the lidar-ratio grows from ~35 to 60 sr in the Figure 6. This increase in the lidar-ratio is a manifestation of the hygroscopic growth due to increased relative humidity as we reach the cloud base. This is consistent with aerosol model properties. For example, a lidar-ratio increase is shown in Figure 7 where we use the OPAC urban aerosol model [14]. Addition of background non-urban aerosols mixed in has the tendency to reduce the lidar-ratio magnitude and growth making agreement even better. Further analysis of the aerosol cloud interaction requires the receipt of the microwave radiometer (MIDAC MW-3000P) which together with the MFRSR can provide the tools needed to improve the work of aerosol-cloud interaction [15]: 1) better RH profiles in which to assess hygroscopic aerosol properties below clouds; 2) near direct liquid water path which combined with cloud optical depth gives droplet diameters.

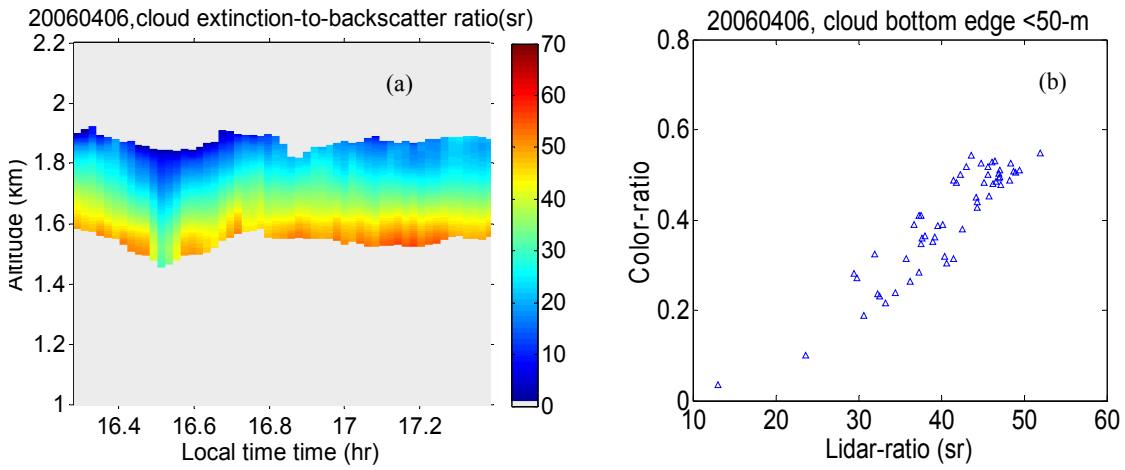

Figure 5. (a) Cloud lidar-ratio and (b) correlation beteen lidar-ratio and color ratio near the cloud bottom.

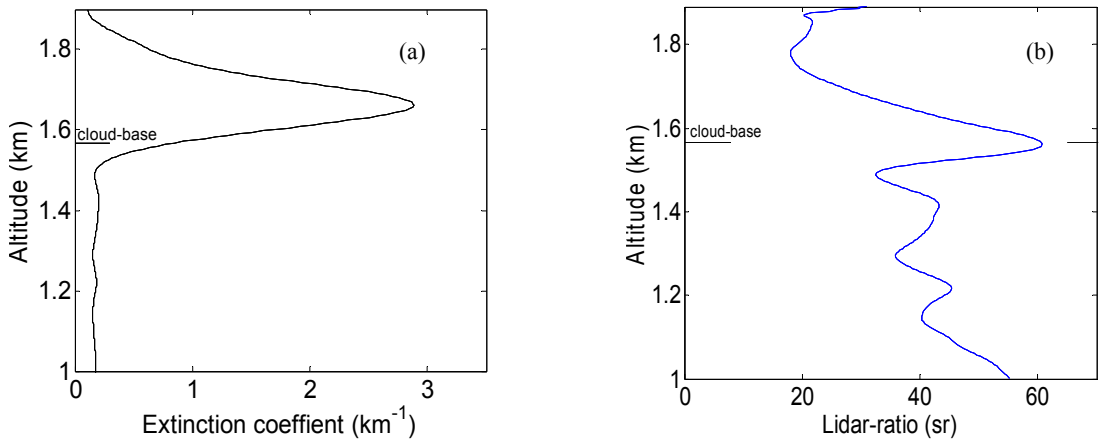

Figure 6. (a) Aerosol and cloud extinction coefficient and (b) lidar-ratio on April 6, 2006.

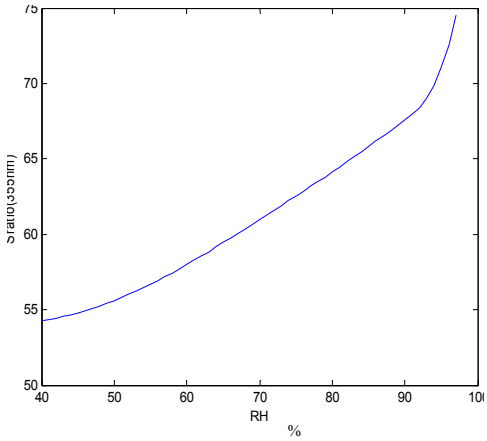

Figure 7. Lidar-ratio (S-ratio) dependence on the relative humidity (RH, %) from the OPAC model.

4. SUMMARY

In this study, we first analyze the retrieval accuracy of cloud extinction from the Raman lidar measurement. Due to the dramatic irregular slopes of N_2-Raman returns at the cloud edges, the common algorithms will result in the large bias on the retrieved extinction at the cloud edges which includes the linear (1^{st} order) and 2^{nd} order polynomial regressions with the N_2-Raman signal and the wide regression range. We find that high-order (≥3) polynomial regression and small regression range are indicated to have better retrieval accuracy of extinction at the cloud edges. In addition, lidar-ratio, color ratio and extinction ratio of water cloud are calculated with the gamma distribution of cloud droplet size and Mie-theory. The results indicate the significant variation and good correlation among them for small droplets, which indicate that we can derive the small droplet size information from the multiple-wavelength Raman lidar measurement. Finally, measurement examples by CCNY multiple-wavelength elastic-Raman lidar of the lidar-ratio and color-ratio at the cloud edges indicate the formation of small droplets. In addition, we also note the increase in aerosol lidar-ratio (S-ratio) below cloud indicative of hygroscopic growth. This work preliminarily verifies the potential of the multiple-wavelength elastic-Raman lidar to investigate the low-level cloud properties and the interaction of aerosol and cloud and awaits more direct verification with a soon to be acquired microwave radiometer.

ACKNOWLEDGEMENTS. This work is partially supported by the research projects of NOAA-CREST #NA17AE1625 and NOAA-ISET #NA06OAR4810187.

REFERENCES

[1] Su, W., G. L. Schuster, N. G. Loeb, R. R. Rogers, R. A. Ferrare, C. A. Hostetler, J. W. Hair, M. D. Obland, "Aerosol and cloud interaction observed from high spectral resolution lidar data," *J. Geophys. Res.*, **113**, D24202 (2008).

[2] Clayton, Marian B., R. Ferrare, D. Turner, R. Newsom, C. Sivaraman, "CART Raman lidar aerosol and water vapor measurements in the vicinity of clouds," *Proc. of 24th International Laser Radar Conference*, P483-385 (2008).

[3] Verghese, Sachin J., A. H. Willitsford, C. R. Philbrick, "Raman lidar measurements of aerosol distribution and cloud properties," *Proc. of SPIE,* Vol. 5887, 100-107 (2005).

[4] Garrett, T. J., P. V. Hobbs, L. F. Radke, "High aitken nucleus concentrations above cloud tops in the Arctic," *J. Atmos. Sci., **59**,* 779-783 (2002).

[5] Russo, Felicita, David N. Whiteman, Belay Demoz, Raymond M. Hoff, "Validation of the Raman lidar algorithm for quantifying aerosol extinction," *Appl. Opt.,* **45**, 7073-7088 (2006).

[6] Whiteman, D. N., "Application of statistical methods to the determination of slope in lidar data," *Appl. Opt.*, **38 (15)**, 3360-3369 (1999).

[7] Pappalardo, G., A. Amodeo, M. Pandolfi, U. Wandinger, et al., "Aerosol lidar intercomparison in the framework of the EARLINET project. 3. Raman lidar algorithm for aerosol extinction, backscatter, and lidar ratio," *Appl. Opt.,* **43**, 5370-5385 (2004).

[8] Wu, Yonghua, Chaw, S., Gross, B., Moshary, F., Ahmed, S., "Low and optically thin cloud measurements using a Raman-Mie lidar," *Appl. Opt.,* **48**:6, 1218 (2009).

[9] Hoff, R. M., et al., "Regional East Atmospheric Lidar Mesonet: REALM," *Proc. of 21st ILRC*, P281-284 (2002).

[10] O'Connor, E. J., A. J. Illingworth, R. J. Hogan, "A technique for autocalibration of cloud lidar," *J. Atmos. Ocean Tech.,* **21(5)**, 777-778 (2004).

[11] Wu, Yonghua, Chaw, S., Gross, B., Moshary,F., Ahmed, S., "Comparison of lidar calibration at 1064-nm channel using the water-phase and cirrus clouds," *Proc. of SPIE*, Vol. 7479, DOI: 10.1117/12.830643 (2009).

[12] Miles, N. L., J. Verlinde, E. E. Clothiaux, "Cloud droplet size distributions in low-level stratiform clouds," *J. Atmos. Sci.,* **57**, 295−311 (2000).

[13] Eberhard, W. L., "CO_2 lidar technique for observing characteristic drop size in water cloud," *IEEE Trans. Geosci Remote Sensing,* **31** (1), 57-63 (1993).

[14] Hess, A. M., P. Koepke, I. Schult, "Optical properties of aerosol and clouds: the software package OPAC," *Bull. Am. Meteorol. Soc.* **79**, pp. 831–844 (1998).

[15] Feingold, G., W. L. Eberhard. D. E. Lane, and M. Previdi, "First measurements of the Twomey aerosol indirect effect using ground-based remote sensors," *Geophys. Res. Lett.,* 30 (6), 1287 (2003).